

Performance Evaluation of DC-DC Boost Converter and its Nonlinear Analysis in Photovoltaic Based System

G. Laxman Manoj¹, K. Durgendra Kumar²

^{1,2}*Department of Electrical and Electronics Engineering, Aditya Engineering College, Surampalem, A.P., India*

Abstract - DC-DC converter is one of the main components in renewable energy generation system. DC-DC converter is nonlinear entity which exhibits nonlinear characteristics. The understanding of Mathematical analysis of PV system and nonlinear dynamics of DC-DC Boost converter is of prime importance. The Performance Evaluation of Boost Converter in a PV based system under different Irradiation levels at constant temperature was studied in this paper. Detailed design of DC-DC Boost Converter dynamics has been provided. The Nonlinear dynamics of DC-DC Boost Converter with different bifurcation parameters is analyzed with the help of Matlab Simulink.

Index Terms - PV cell, Maximum power point tracking, Boost converter, Bifurcation.

I. INTRODUCTION

Electricity generation is one of the most fundamental challenge of the world. To generate electricity, thermal power plant, hydro power plant and nuclear power plant are used. These are the conventional method to generate electricity. But there are limitations in the conventional methods. Therefore, renewable energy sources are preferred to generate electricity. Renewable energy sources which contain geothermal, ocean, biomass, solar, wind and hydropower have a huge capability to deliver necessary energy needs for the world. The main advantage of Renewable energy sources that it can be utilized without the emission of harmful pollutants. Among the renewable sources, photovoltaic system is one of the most widely used method to generate sustainable electricity.

Photovoltaic system is most widely used source for power generation. It has various advantages such as simple design, low maintenance and ecofriendly system. The main disadvantage of Photovoltaic system is high initial cost and poor efficiency.

PV cell is the basic element responsible for generation of electricity from light. It is necessary to accurately model the dynamic behaviour of PV array for understanding of PV system characteristics. In [4], the authors have provided a detailed interpretation of solar PV cell characteristics. The physical parameters which influence it have also been explained. But the main focus was the choice of two terms of the Double Exponential equation, describing the I-V curve of the cell precisely. The entire work was performed for the solar PV cell, used in space and therefore accuracy was the driving factor regardless of complexity. In [1], the authors investigated different climatic conditions such as humidity level, variable irradiation level, temperature and dust accretion in the modelling of a realistic PV system.

DC-DC converter is used to control the operating point of PV system thereby operating PV panel at MPP to draws maximum power to the load. The performance and conversion efficiency of the PV system is truly dependent on control strategy of DC-DC converters. A detailed investigation of different design aspects of DC-DC converter in renewable generation concept has been investigated by [2]. A wide variety of converters have been taken into consideration and different losses of the converters have been evaluated. A comprehensive review of stability of different DC-DC converter have been discussed in [5].

A MPPT is very effective technique which helps to obtain the optimal power by measuring and sampling the output voltage or current of the solar array and then controlling a power converter or adjusting the load to make sure that maximum power is delivered to the system load for any given atmospheric condition.

A various MPPT Methods are used to obtain maximum power from PV system are listed below.

- P&O Algorithm
- Incremental conductance (IG) Technique

- Fraction open circuit Technique
- Fractional short circuit current Technique
- Fuzzy logic Technique

All these techniques yield better response to the variations of irradiance and temperature of the PV panel. Among them, P&O MPPT is most simple and effective technique to obtain maximum power at constant temperature and varying irradiance. A proper classification and comparative analysis of different MPPT algorithms have been studied in [6–10]. In [11], the authors presented that majority of these bifurcation are considered as “border collision bifurcation”. The local bifurcation structure is predicted through formation of a normal form. This form of procedure is valid for many power electronic circuits and other piecewise smooth systems.

The rest of the paper is categorized as follows

The next Section 2 describes the mathematical modelling and analysis of PV panel and P&O MPPT method which is used in simulation to extract optimal power from the Photovoltaic system. Section 3 elaborates DC-DC Boost converter design aspects and integration of MPPT control of Boost converter with PV System. Section 4 includes simulation results of PV system for different irradiance conditions at constant temperature and Bifurcation and Chaos results of DC-DC Boost converter. Section 5 with conclusion remarks.

II. MODELLING AND ANALYSIS OF PHOTOVOLTAIC SYSTEM

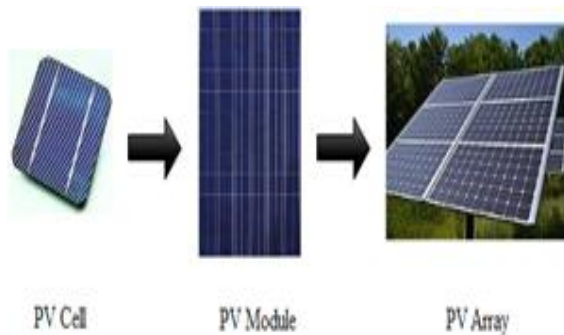


Fig 2.1: Elements of Solar PV System

A. Model of Solar Cell

Fig 2.2 represents the equivalent circuit of a single diode model of PV cell. The ideal model of PV cell has

a constant current source and a diode whereas the practical one has additional series resistance R_s and parallel resistance R_p .

$$I = I_{pv} - \frac{V+IR_s}{R_p} - I_d \left[\exp\left(\frac{V+IR_s}{\frac{akT}{q}}\right) - 1 \right] \quad (2.1)$$

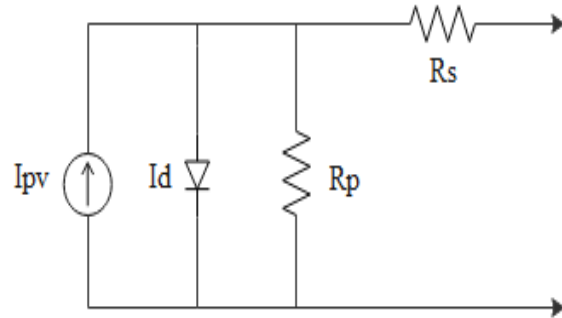


Fig 2.2: Single diode model of PV cell

There are different mathematical models of solar cell which is compared in [3].

B. Three-Parameter Model

In this model, $R_s = 0$ and $R_p = \infty$

$$I = I_{pv} - I_d \left[\exp\left(\frac{V}{\frac{akT}{q}}\right) - 1 \right] \quad (2.2)$$

$$I = n_p \left[I_{pv} - I_d \left[\exp\left(\frac{V}{\frac{ns}{akT}}\right) - 1 \right] \right] \quad (2.3)$$

$$I = I_{sc,ref} \left(\frac{S}{S_{ref}}\right) (I_{sc,ref} + \alpha_{isc} \Delta T) \quad (2.4)$$

$$I_d = I_{d,ref} \left(\frac{T}{T_{ref}}\right)^3 \exp\left(\frac{qE_G}{k} \left(\frac{1}{T_{ref}} - \frac{1}{T}\right)\right) \quad (2.5)$$

C. P&O MPPT

Perturb & Observe (P&O) MPPT is a simple, effective and easy to implement technique. It controls by changing yield voltage at uniform intervals and thereby matches the PV output power with earlier sample value. Moreover, earlier information of the PV panel characteristics is not needed. In its clarity form, this technique usually delivers better performance for smaller deviation in solar irradiation. The classic perturbs and observe (P&O) method has one downside of mediocre performance at low solar irradiation. Fig 2.3 demonstrates the flow chart of P&O MPPT algorithm.

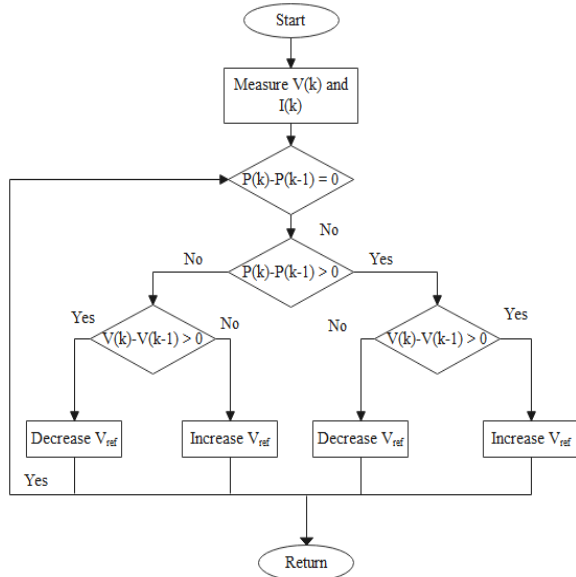


Fig 2.3: P&O MPPT algorithm

III. DC-DC BOOST CONVERTER

The duty cycle of boost converter is represented as

$$\frac{V_o}{V_{in}} = \frac{1}{1-d} \quad (3.1)$$

The selection of inductor L and capacitor C of boost converter can be evaluated from below procedure.

Step 1: Sense the values of P_{mpp} , V_{mpp} , I_{mpp} , I_{sc} .

Step 2: If internal losses of converter is zero then output voltage will be

$$V_{in}I_{in} = V_oI_o = \frac{V_o^2}{R_L} = P_{mpp} \quad (3.2)$$

$$\frac{V_o^2}{R_L} = P_{mpp} = V_o = \sqrt{P_{mpp} * R_L} \quad (3.3)$$

Step 3: The duty of converter at given output voltage will be

$$V_o = \frac{V_{in}}{1-D} = D = 1 - \frac{V_{in}}{V_o} \quad (3.4)$$

Step 4: The current through the inductor is given by

$$I_L = \frac{V_{in}}{(1-D)^2 R_L} \quad (3.5)$$

If the deviation of inductor current I_L is 5% then

$$\Delta I_L = 0.05 * I_L \quad (3.6)$$

Since,

$$\Delta I_L = \frac{V_{in}D}{L f_s} \quad (3.7)$$

Evaluate L from the above equation.

Step 5: The maximum value of inductor current is evaluated by

$$I_{Lmax} = I_L + \frac{\Delta I_L}{2} \quad (3.8)$$

The minimum value of inductor current is evaluated by

$$I_{Lmin} = I_L - \frac{\Delta I_L}{2} \quad (3.9)$$

Step 6: If the ripple is less than 1% then the input and output capacitance values are

$$C_o = \frac{D}{R_L f_s \frac{\Delta V_o}{V_o}} \quad (3.10)$$

$$C_{in} = \frac{D}{0.01 * R_L f_s^2 L} \quad (3.11)$$

A. PV Panel integrated with DC-DC Boost Converter

Fig 3.1 represents the block diagram of DC-DC converter integrated with PV panel and perturb and observe MPPT control logic.

The PV Panel 1Soitech 1STH-230-P is used which consists of 1 Parallel string having 1 Series connected modules per string, each module contains 60 cells. The DC-DC Boost converter is chosen which is connected between PV panel and load.

The MPPT tracking and relevant control measures the PV panel voltage V_{pv} and PV panel current I_{pv} and generates duty cycle with respect to maximum power point which needs to be maintained. This Duty cycle is fed to PWM scheme which provides the necessary control action of the boost converter. A gate drive circuit is used to provide necessary PWM to the switch of the boost converter.

Photovoltaic Module

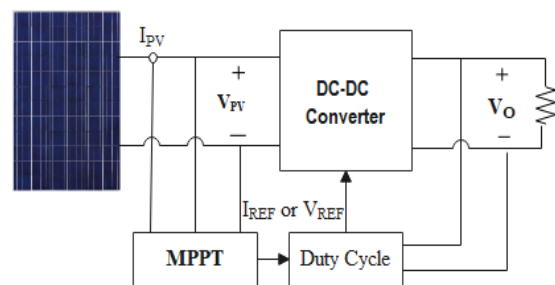


Fig 3.1: Block diagram of DC-DC converter integrated with PV panel and MPPT control logic.

IV. SIMULATION RESULTS

MATLAB-Simulink has been used to simulate the PV based DC drive system. The P-V and V-I

characteristics of the PV module under Non-uniform irradiance and Non-uniform temperature are shown in Fig 4.1(a) and Fig 4.1(b) respectively. The $V-I$ and $P-V$ characteristics are not linear in nature and the MPPT algorithm provides the maximum power point. There are parameters of Soltech 1STH-230-P, PV module shown below

Table 4.1: Simulation Parameters

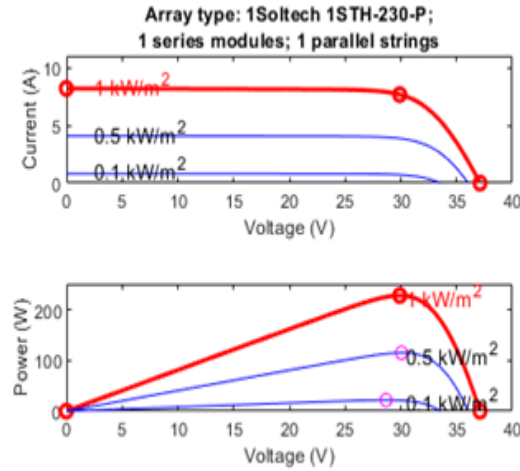
Parameters	Values
Power of PV module	228.735W
Number of series connected PV module	1
Number of parallel connected PV module	1
Open-circuit voltage	37.1 V
Short circuit current	8.18 A
Voltage at maximum power point	29.9 V
Current at maximum power point	7.65 A

The DC-DC Boost converter is coupled between PV panel, MPPT P&O controller and load. The boost converter used in the Simulink model level up the input voltage of 30.24V to output voltage of 67.35V with duty cycle of 54.46% at solar irradiance of 1000W/m² and temperature of 25°C is applied to the PV module. Using MPPT perturb and observe Technique, maximum power of 226.8W at maximum power point is obtained. Three different solar irradiances levels i.e., uniform irradiation of 1000W/m², Ramp increase in solar irradiance and Non-uniform solar irradiance at constant temperature are applied to the PV module.

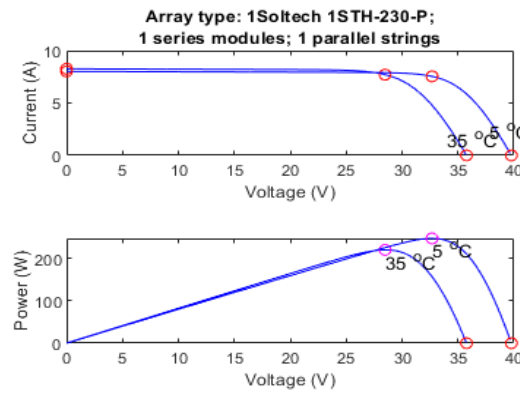
Fig 4.2(a) and Fig 4.3(a) shows performance of PV module without and with P&O MPPT under uniform solar irradiation level. Performance of PV module with P&O MPPT delivers maximum power of 226.8W compared to 225.5W of the PV module without MPPT. Fig 4.2(b) and Fig 4.3(b) shows performance of PV module without and with P&O MPPT under Ramp increase in solar irradiation level. Performance of PV module with P&O MPPT delivers maximum power of 226.8W compared to 222.8W of the PV module without MPPT. Fig 4.2(c) and Fig 4.3(c) shows performance of PV module without and with P&O MPPT under Non-uniform solar irradiation levels. Performance of PV module with P&O MPPT delivers maximum power of 221.9W compared to 88.56W of the PV module without MPPT. The Simulink model of PV System with P&O MPPT technique delivers great response under varying solar

irradiation levels at constant temperature of 25°C have been Studied.

The performance of PV system under these varying irradiation levels using P&O MPPT technique are observed and results have been analyzed with below graphs.

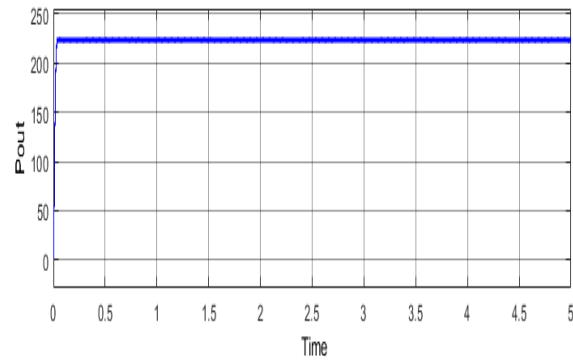


(a)

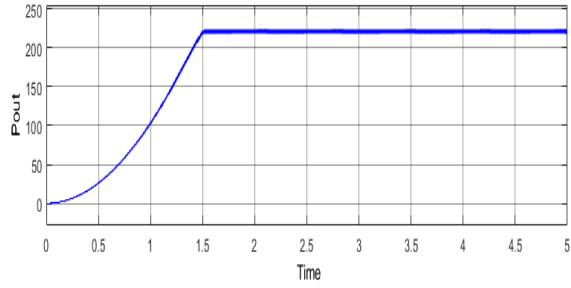


(b)

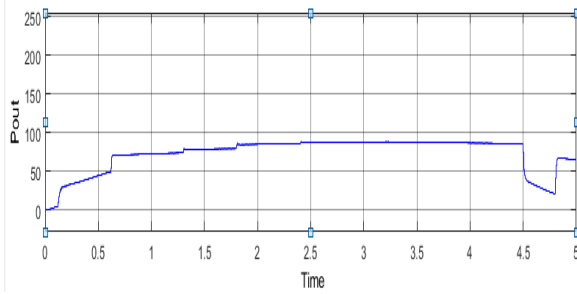
Fig 4.1: (a) $I-V$ and $P-V$ characteristics of PV array with Non-uniform irradiance (b) $I-V$ and $P-V$ characteristics of PV array with Non-uniform temperature



(a)



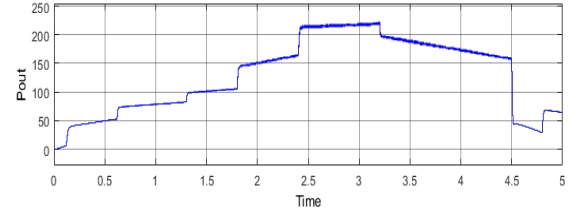
(b)



(c)

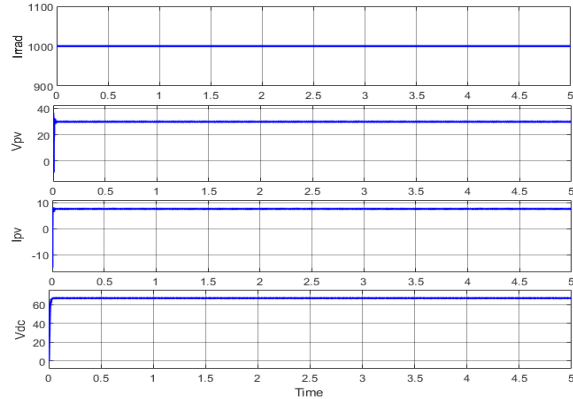
Fig 4.2: Maximum power transfer of PV array without P&O MPPT(a) Uniform irradiance (b) Ramp increase in irradiance (c) Non-Uniform irradiance.

Fig 4.3(a) shows the performance of perturb and observe MPPT with uniform solar irradiance. Fig 4.3(b) illustrates performance of MPPT with ramp increase in solar irradiance. Fig 4.3(c) shows the performance of MPPT with non-uniform solar irradiance.

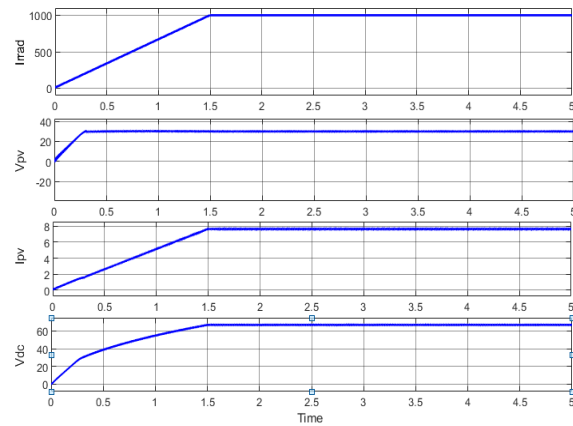


(c)

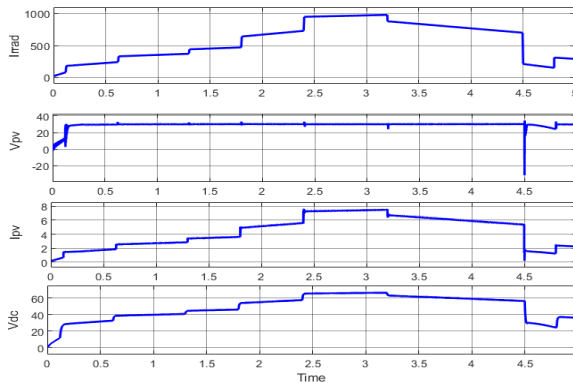
Fig 4.3: Maximum power transfer of PV array with P&O MPPT(a) Uniform irradiance (b) Ramp increase in irradiance (c) Non-Uniform irradiance



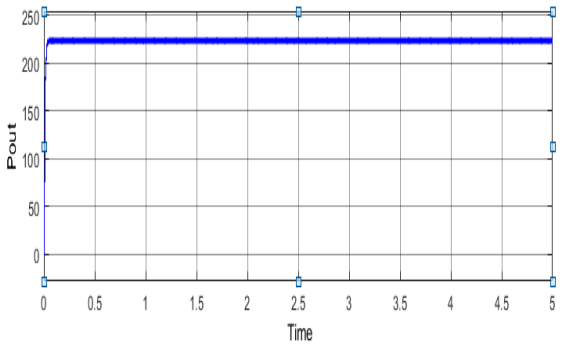
(a)



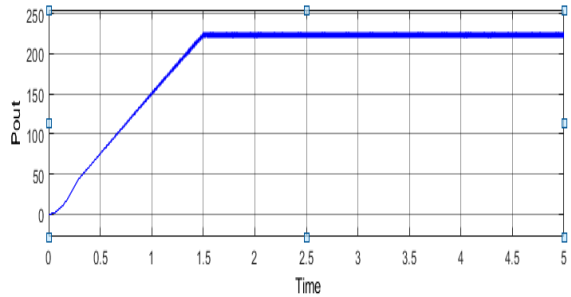
(b)



(c)



(a)



(b)

Fig 4.4: Output characteristics of PV array with P&O MPPT

- (a) Uniform irradiance (b) Ramp increase in irradiance
- (c) Non-Uniform irradiance.

A. Non-linear Analysis of Boost Converter

For analysis of the behaviour of the converter, iterative map is developed. The difference equation of the system can be described as

$$x_{n+1} = f(x_n, \alpha), x \in \mathbb{R}^N, \alpha \in \mathbb{R} \quad (4.1)$$

where

$$x = [i_L \quad V_c]^T \quad (4.2)$$

i_L is the inductor current and V_c is the capacitor voltage

The converter circuit has two states as follows.

When switch is closed, the equations governing of the converter condition can be written as

$$\begin{cases} L \frac{di_L}{dt} = V_{in} & S = \text{closed} \\ C \frac{dv_c}{dt} = \frac{-v_c}{R} & S = \text{closed} \end{cases} \quad (4.3)$$

The solution of the above equation is represented as

$$\begin{cases} t_n = \frac{L(I_{ref} - i_n)}{V_{in}} \\ V_c(t_n) = V_n \exp\left(\frac{-t_n}{RC}\right) \end{cases} \quad (4.4)$$

When switch is open, the equations governing of the converter condition can be written as

$$\begin{cases} L \frac{di_L}{dt} + v_c = V_{in} & S = \text{open} \\ C \frac{dv_c}{dt} + \frac{v_c}{R} = \frac{-v_c}{R} & S = \text{open} \end{cases} \quad (4.5)$$

The dynamics can be defined as second order differential equation which can be represented as

$$\frac{d^2}{dt^2}(i_L) + \left(\frac{1}{RC}\right) \frac{d}{dt}(i_L) + \left(\frac{1}{LC}\right)(i_L) = \frac{V_{in}}{LCR} \quad (4.6)$$

The roots of homogeneous equation can be represented as

$$\lambda_{1,2} = \frac{1}{2RC} \pm \sqrt{\frac{1}{4R^2C^2} - \frac{1}{LC}} \quad (4.7)$$

$$\lambda_{1,2} = -\frac{1}{2\tau_{RC}} \pm j\omega \quad (4.8)$$

where

$$\omega = \sqrt{\frac{1}{LC} - \frac{1}{(2\tau_{RC})^2}} \quad (4.9)$$

The solution of homogeneous equation can be represented as

$$i_L(t) = \exp\left(\frac{-t}{2\tau_{RC}}\right) (a_1 \sin \omega t + a_2 \cos \omega t) + \frac{V_{in}}{R} \quad (4.10)$$

Where

$$a_1 = \frac{\frac{L}{2\tau_{RC}}(I_{ref} - \frac{V_{in}}{R}) + V_{in} - v_n \exp\left(\frac{-t_n}{\tau_{RC}}\right)}{\omega L} \quad (4.11)$$

$$a_2 = I_{ref} - \frac{V_{in}}{R} \quad (4.12)$$

Fig 4.5 shows the flow chart of bifurcation phenomena in Boost converter. The bifurcation nature of the boost converter by varying inductor current and input voltage has been analysed in Fig 4.6 and Fig 4.7 respectively.

The bifurcation analysis of the boost converter under reference current as bifurcation element is plotted in fig 4.6.

The reference current I_{ref} increases gradually with a step change of 0.5A with respective to change in the inductor current. The other elements are considered to be fixed which are input voltage of 20V, load resistance of 20 Ω , capacitance 100 μ F, inductance 28mH and clock frequency of 500 Hz.

The fig 4.6 shows at 2.25A, 3.49A and 3.8A I_{ref} values, the converter undergoes period-doubling phenomenon. At 3.49A, the two viewpoints are observed and shows a difference as one clock pulse in each cycle that does not perform a switching action. The Converter enters into Chaotic region from 3.8A and exhibits small periodic orbits at larger values of reference current.

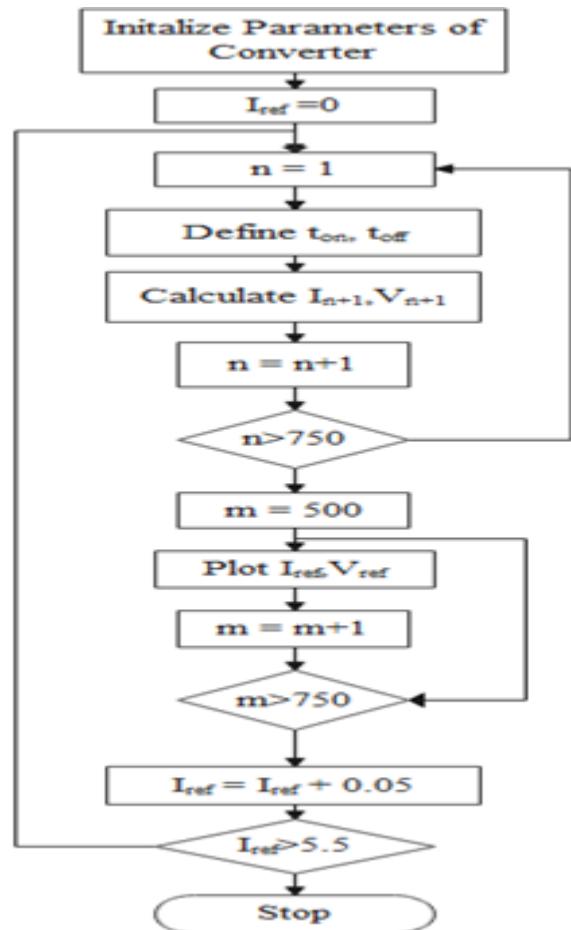


Fig 4.5: Flow chart of bifurcation phenomenon in Boost converter.

The fig 4.7. shows bifurcation nature of the boost converter by taking input voltage as bifurcation element. The input voltage varies gradually with a step change of 10V from 10 to 70V in accordance with change in inductor current. The other elements are considered to be fixed which are load resistance of 20 Ω, capacitance 100μF, inductance 28mH, I_{ref} of 5A and clock frequency of 500 Hz.

The boost converter exhibit period-doubling phenomenon from 32V and enters into chaos as input voltage is increased beyond 49V. A sudden change of behaviour occurs at 32V leads converter to enter into period 2 from period 1. At 49V, the period 2 behaviour is again dividing into period 3. This is caused by arrival of pulse before the current value becomes I_{ref} during on time.

At that point of time, four clock pluses are present in a cycle, however the orbit is in phase period 3. In the Chaotic region, small periodic windows are present which are having period-doubling cascade behaviour.

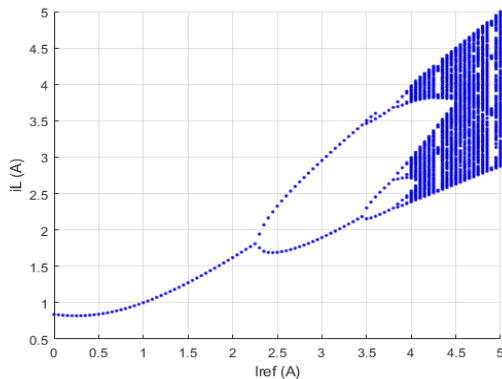


Fig 4.6: Bifurcation due to change in inductor current

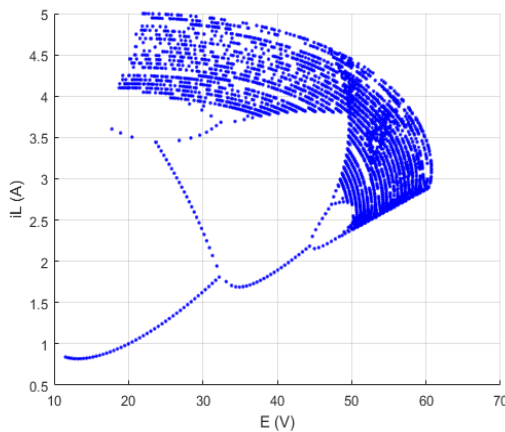


Fig 4.7: Bifurcation due to change in input voltage

V. CONCLUSION

The aim of this paper has been to conduct research into high efficiency standalone PV systems. Mathematical analysis of PV system, DC-DC converter has been provided in this work. Detailed design aspects of boost converter have been carried out. Non-linear analysis of boost converter has been analysed in this paper. Bifurcation and chaos have been analysed in this work. Different simulation results have been presented.

REFERENCES

- [1] Gupta, Ankit, Yogesh K. Chauhan, and Rupendra Kumar Pachauri. "A comparative investigation of maximum power point tracking methods for solar PV system." *Solar energy* 136, 2016: 236-253.
- [2] Sivakumar, S., et al. "An assessment on performance of DC–DC converters for renewable energy applications." *Renewable and Sustainable Energy Reviews* 58, 2016: 1475-1485.
- [3] Baig, Mirza Qutab, Hassan Abbas Khan, and Syed Muhammad Ahsan. "Evaluation of solar module equivalent models under real operating conditions—A review." *Journal of Renewable and Sustainable Energy* 12.1, 2020: 012701.
- [4] Wolf, M., G. T. Noel, and Richard J. Stirn. "Investigation of the double exponential in the current—voltage characteristics of silicon solar cells." *IEEE Transactions on electron Devices* 24.4, 1977: 419-428.
- [5] Siewniak, Piotr, and Bogusław Grzesik. "A brief review of models of DC–DC power electronic converters for analysis of their stability." *International Journal of Electronics* 101.10, 2014: 1405-1426.
- [6] Gupta, Ankit, Yogesh K. Chauhan, and Rupendra Kumar Pachauri. "A comparative investigation of maximum power point tracking methods for solar PV system." *Solar energy* 136, 2016: 236-253.
- [7] Bendib, Boualem, Hocine Belmili, and Fateh Krim. "A survey of the most used MPPT methods: Conventional and advanced algorithms applied for photovoltaic systems." *Renewable and Sustainable Energy Reviews* 45, 2015: 637-648.
- [8] Subudhi, Bidyadhar, and Raseswari Pradhan. "A comparative study on maximum power point tracking techniques for photovoltaic power

- systems." IEEE transactions on Sustainable Energy 4.1, 2012: 89-98.
- [9] Rezk, Hegazy, and Ali M. Eltamaly. "A comprehensive comparison of different MPPT techniques for photovoltaic systems." Solar energy 112 2015: 1-11.
- [10] Esham, Trishan, and Patrick L. Chapman. "Comparison of photovoltaic array maximum power point tracking techniques." IEEE Transactions on energy conversion 22.2, 2007: 439-449.
- [11] Yuan, Guohui, et al. "Border-collision bifurcations in the buck converter." IEEE Transactions on Circuits and Systems I: Fundamental Theory and Applications 45.7, 1998: 707-716.